Biophysical Chemistry 24 (1986) 121–133
Elsevier

BPC 01060

DISPLACEMENT OF SODIUM IONS BY SURFACTANT IONS FROM DNA

A ^{23}Na-NMR INVESTIGATION

A. DELVILLE [a], P. LASZLO [a,*] and R. SCHYNS [b]

[a] *Laboratoire de chimie organique physique and* [b] *Laboratoire de biochimie, Université de Liège au Sart-Tilman, 4000 Liège, Belgium*

Received 25th September 1985
Revisal manuscript received 27th December 1985
Accepted 10th April 1986

Key words: DNA; ^{23}Na-NMR

^{23}Na-NMR probes the ionic composition in the immediate vicinity of the DNA molecule, in the presence of a series of quaternary ammonium bromides, of varying hydrocarbon chain length. The ^{23}Na-NMR line shows two Lorentzian components, in accordance with quadrupolar relaxation theory for $S = 3/2$ nuclei under slow modulation. Deconvolution of the observed lineshape provides, in a reliable manner, the relative fraction of sodium counterions neutralizing the phosphate sites on DNA. This quantity ($p_B X^2$) serves as an index of the relative affinities of various surfactant ions toward DNA, Na^+ being the reference cation. The results are consistent with site binding of detergent ions to the nucleic acid, an interaction dominated by hydrophobic forces.

1. Introduction

Many studies of ion-polyelectrolyte interactions have focussed upon surfactant counterions [1,2]. These are strong interactions: the solubility [3] and conformation [4] of the polymer are affected. A recent noval electrochemical determination of the activity of surfactant ions in the presence of various polyelectrolytes has been quite fruitful [2,4–6]. Accordingly, one of us has modelled the interaction between the sodium salt of DNA and the dodecyltrimethylammonium ion [7], hereafter referred to as $(NMe_3Do)^+$.

This model computes the extent of ionic condensation [8], and takes into account cooperative site binding [9] due to intense hydrophobic interactions [7] between surfactant molecules attached to adjoining sites. The present study concerns itself with interactions involving NaDNA and a series of quaternary ammonium salts Q^+Br^-, where the cation

$$Q^+ = N(n\text{-}C_3H_7)_4^+ \quad (NPr_4^+)$$
$$= N(n\text{-}C_4H_9)_4^+ \quad (NBu_4^+)$$
$$= N(n\text{-}C_5H_{11})_4^+ \quad (NPe_4^+)$$
$$= N(n\text{-}C_6H_{13})_4^+ \quad (NHex_4^+)$$
$$= N(CH_3)_3(n\text{-}C_{12}H_{25})^+ \quad (NMe_3Do^+)$$

The tool of this study is ^{23}Na-NMR [10,11]. By contrast with electrochemical determinations of the ionic activity, determined predominantly by the ionic composition at large distances from the polyelectrolyte [8,12], the observed linewidth for the quadrupolar ^{23}Na nucleus is directly driven by the ionic composition at very short distances, right next to the polymeric surface [13–15]. This useful feature, of quadrupolar relaxation reflecting the local distribution of ions in close contact with the

* To whom correspondence should be addressed.

polyelectrolyte, has been put to advantage in a number of ^{23}Na-NMR studies of the interaction of counterions with DNA [16–20] or synthetic polyions [21–26].

2. Experimental

2.1. Materials

Calf thymus DNA (Sigma) is first dissolved in 0.1 M aqueous NaCl solution containing 1 mM EDTA at pH 7.5. The approx. 3% (w/w) proteins are eliminated by incubation at 37°C for 2 h in 100 μg/ml proteinase K solution, followed by treatment with a 24:1 binary mixture of chloroform and isoamyl alcohol. After centrifugation, the aqueous phase is precipitated with cold ethanol (−20°C) and then redissolved in 0.1 M NaCl, 1 mM EDTA solution buffered at pH 7.5. In order to prepare a DNA solution containing the minimum amount of extraneous ions, we again precipitate the DNA solution with technical ethanol, prior to dissolving the precipitate in 0.1 M NaCl solution. This last solution, after sonication, undergoes three series of cold technical ethanol (−20°C) precipitations, followed by mixing with a water/ethanol (20:80) mixture. At each step, DNA is redissolved in 0.1 M NaCl solution. Finally, we dissolve the air-dried DNA precipitate in an ion-free water solution.

The concentration of phosphate sites is measured from the absorbance at 260 nm ($c_p = 15$ mM), and this value is checked from a DABA determination. The Na^+ concentration was determined using atomic absorption as $[Na^+] = 18 \pm 0.5$ mM. The pH of this stock solution of DNA is 6.11 ± 0.1. The molecular weight of DNA after sonication is determined as approx. 6×10^6 by viscosimetry [27]. No denaturation occurs up to 60°C, as shown by measurements of the absorbance (260 nm) as a function of temperature. All the glassware used for storage and for studying Q^+-DNA interactions has been pretreated with boiling EDTA (≅ 0.1 M) solutions in order to remove metallic cations from the glass walls.

The quaternary ammonium salts NPr_4Br, NBu_4Br, NPe_4Br (Aldrich), $NHex_4Br$ (Ventron) and NMe_3DoBr (Sigma) first underwent azeotropic distillation with *n*-hexane. They were then dissolved in acetone, ethyl acetate, or diethyl ether, and filtered from the solutions. After recrystallization, the salts are rinsed with *n*-hexane, and then dried under vacuum (≅ 5×10^{-2} mmHg) for 3–4 h. They are kept under vacuum in a desiccator. For NMR measurements, NaCl (suprapure, Merck) was used without further purification.

2.2. Methods

^{23}Na-NMR spectra are obtained on solutions containing 10% ^2H_2O for the lock and at 303 ± 0.5 K with a Bruker AM 300 WB spectrometer at a Larmor frequency of 79.391 MHz. An acquisition time of 2 h was necessary for a satisfactory signal-to-noise ratio ($S/N > 80$) with 1.5 mM NaDNA solution. Solutions of DNA in the presence of various salts required much smaller acquisition times, since the linewidths were smaller, in accordance with the Ernst-Anderson formula. Longitudinal relaxation times (T_1) were measured with the standard (180°–*t*–90°) sequence, followed by a non-linear regression on at least 10 different determinations for variable delays *t*. The 90° pulse had a duration of 12.8 μs. The transverse relaxation times (T_2) were simply evaluated from the linewidths at half-height: $\Delta\nu_{1/2} = (\pi T_2)^{-1}$. The lineshape was numerically deconvoluted into the two-component Lorentzian absorptions, using an Apple II microcomputer, with a generalized Newton-Gauss minimization procedure.

3. Interpretation of the results

We have plotted in fig. 1 the changes in ^{23}Na relaxation rates as a function of addition of NaCl, at constant DNA concentration. A first interesting observation is the coexistence of two components, fast (f) and slow (s), for transverse magnetization, which we were thus encouraged to separate by deconvolution. Quadrupolar relaxation theory indicates that for an $S = 3/2$ nucleus transverse magnetization obeys the following equations [28]:

$$M_x = M_x^0 \left[0.6 \exp\left(-\frac{t}{T_{2f}} \right) + 0.4 \exp\left(-\frac{t}{T_{2s}} \right) \right] \quad (1a)$$

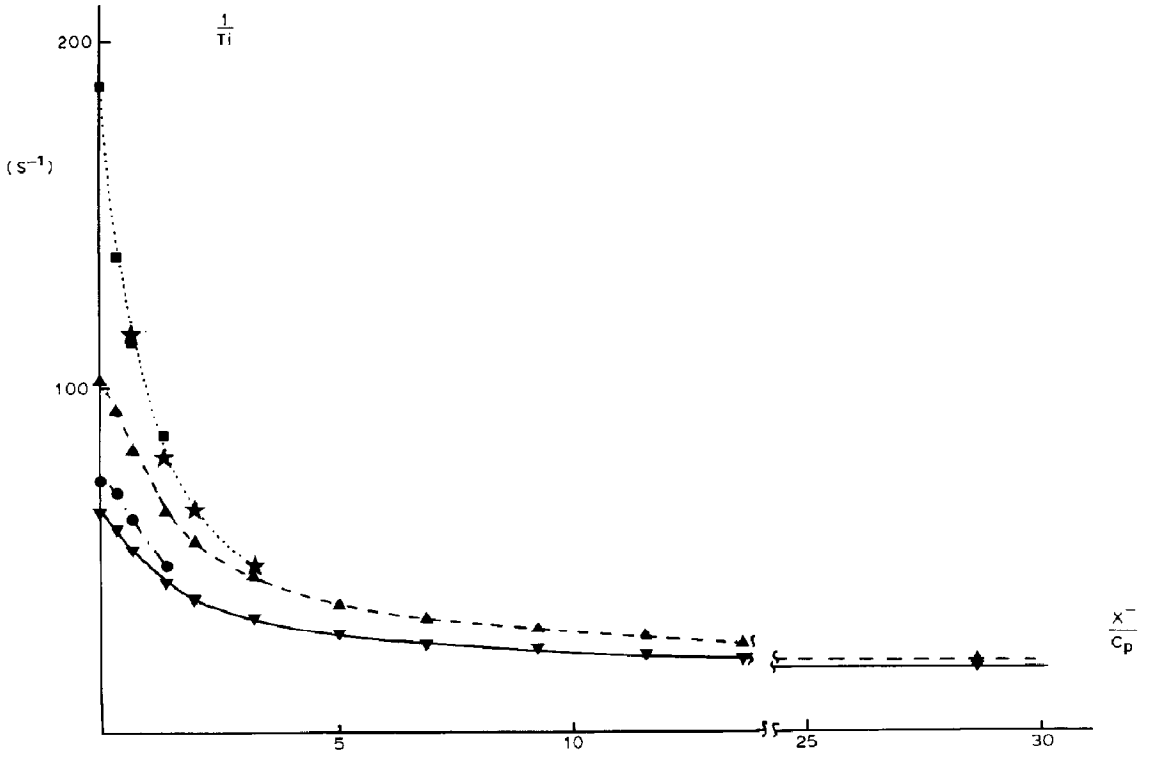

Fig. 1. Variation of the ^{23}Na relaxation rates for an aqueous solution of NaDNA ($c_p = 1.5$ mM) in the presence of added NaCl. The curves passing through the data points are only shown for easier visualization, they have no theoretical significance. (■) $1/T_{2f}$ from lineshape deconvolution. (★) $1/T_{2f}$ from eq. 5. (▲) $1/T_{2app}$. (●) $1/T_{2s}$ from lineshape deconvolution. (▼) $1/T_1$.

with

$$\frac{1}{T_{2f}} = \frac{1}{40}\left(\frac{e^2qQ}{\hbar}\right)^2 [J(0) + J(\omega_0)] \tag{1b}$$

and

$$\frac{1}{T_{2s}} = \frac{1}{40}\left(\frac{e^2qQ}{\hbar}\right)^2 [J(\omega_0) + J(2\omega_0)] \tag{1c}$$

where the spectral densities J have their usual meaning:

$$J(m\omega_0) = \frac{2\tau_c}{1 + (m\omega_0\tau_c)^2} \tag{1d}$$

and where the quadrupolar coupling constant $\chi = (e^2qQ/\hbar)$.

These simplified equations [28] are valid provided that the autocorrelation function for the electrostatic field gradient (efg) can be characterized by a single correlation time, τ_c. Parallel equations describe the longitudinal magnetization [28]:

$$(M_z - M_z^o) = -M_z^o\left[0.8\exp\left(-\frac{t}{T_{1s}}\right) + 0.2\exp\left(-\frac{t}{T_{1f}}\right)\right] \tag{2a}$$

with

$$\frac{1}{T_{1s}} = \frac{1}{20}\left(\frac{e^2qQ}{\hbar}\right)^2 J(2\omega_0) \tag{2b}$$

and

$$\frac{1}{T_{1f}} = \frac{1}{20}\left(\frac{e^2qQ}{\hbar}\right)^2 J(\omega_0) \tag{2c}$$

In practice, when the product $\omega_0\tau_c > 1.5$ the relaxation rates $1/T_{2f}$ and $1/T_{2s}$ differ sufficiently for deconvolution of the lineshape to be reliably performed. However, under the same conditions, the corresponding relaxation rates $1/T_{1f}$ and $1/T_{1s}$ remain close to one another; hence the longitudinal magnetization is deceptive: it appears monoexponential, with a characteristic apparent relaxation rate $1/T_1$ similar to $1/T_{2s}$. This is shown in fig. 1; a similar observation has been made by Levij et al. [25] for polyacrylate. Related observations have also been made by Nordenskiold et al. [20] on various types of DNA at 20.5°C. The resulting relaxation times characterizing our sample of NaDNA are gathered in table 1.

When the fast and slow relaxation rates become similar, deconvolution of the lineshape can no longer be carried out. In practice, with our experimental accuracy (see section 2), this unsatisfactory situation is obtained when the ratio $(\Delta\nu_{1/8}/\sqrt{7}\,\Delta\nu_{1/2})$ falls below 1.08 [29].

However, it can be bypassed: if we take advantage of the similarity between $1/T_1$ and $1/T_{2s}$, we can derive the relaxation rate $1/T_{2f}$ from the apparent value $1/T_2$. Indeed, if one assumes that a single line occurs, this corresponds from eq. 1a to:

$$M_x = M_0 \exp\left(-\frac{t}{T_{2ap}}\right) = M_0\left[0.6\exp\left(-\frac{t}{T_{2f}}\right) + 0.4\exp\left(-\frac{t}{T_{2s}}\right)\right] \tag{3}$$

Rather than using the approximate equation [22]

$$\frac{1}{T_{2ap}} = \frac{0.6}{T_{2f}} + \frac{0.4}{T_{2s}} \tag{4}$$

we start with the Fourier inverse of eq. 3, and we make the empirically justified assumption that it approximates a single Lorentzian according to:

$$\frac{T_{2ap}}{1+(2\pi\nu T_{2ap})^2} = \frac{0.6T_{2f}}{1+(2\pi\nu T_{2f})^2} + \frac{0.4T_{2s}}{1+(2\pi\nu T_{2s})^2}. \tag{5}$$

If one sets eq. 5 at the two frequencies $\nu = 0$ and $\nu = (2\pi T_{2ap})^{-1}$,

$$T_{2f}^3\frac{0.3}{T_{2ap}^2} + T_{2f}^2\frac{0.2T_{2s}}{T_{2ap}^2}\left[\left(\frac{T_{2s}^2}{T_{2ap}^2}-1\right)\left(\frac{T_{2s}^2}{T_{2ap}^2}+1\right)^{-1}\right] - T_{2f}\cdot 0.3 + 0.2T_{2s}\left[\left(\frac{T_{2s}^2}{T_{2ap}^2}-1\right)\left(\frac{T_{2s}^2}{T_{2ap}^2}+1\right)^{-1}\right] = 0 \tag{6}$$

We then proceed to solve eq. 6 by an iterative Newton-Gauss procedure. We obtain T_{2f} in this manner, after setting $T_{2s}^{-1} = T_1^{-1} + 10\ s^{-1}$, by reference to the experimental situation plotted in fig. 1. This determination of the transverse relaxation time T_{2f} requires only measurement of the longitudinal and transverse relaxation times.

The method which we have just described resembles markedly that of Gustavsson et al. [22]; it has the advantage of not requiring linearization of the exponential functions (cf. eq. 3), and the domain of applicability is slightly improved with respect to the literature procedure [22]: to values of the product $\omega_0\tau_c$ below 1.6. As shown in fig. 1, agreement between this new simplified method and the standard deconvolution is excellent.

Let us now assume fast chemical exchange be-

Table 1

Characteristic parameters for the NaDNA sample at 303 ± 0.5 K

c_p [a] (mM)	$[Na^+]$ [a] (mM)	M [a]	T_1 (ms)	T_2 [b] (ms)	T_{2s} [c] (ms)	T_{2f} [c] (ms)	$\sqrt{p}_{BX}$ [d] (kHz)	τ_c [d] (ns)
1.5	1.8	0.6×10^6	15.5	9.8	13.8	5.2	136 ± 10	3.5 ± 1

[a] See section 2.
[b] From the linewidth at half-height.
[c] From deconvolution of the lineshape.
[d] Assuming $p_F/T_{2F} = 30\ s^{-1}$.

Table 2

[NaCl] (mM)	$1/T_1$ (s^{-1})	$1/T_2$ (s^{-1})	$1/T_{2s}$ [a] (s^{-1})	$1/T_{2f}$ [a] (s^{-1})	$\sqrt{p}\chi$ [b] (kHz)	τ_c (ns)	$1/T_{2f}$ [c] (s^{-1})	$\sqrt{p}\chi$ [d] (kHz)	τ_c [d] (ns)
0	64.1	102	73±0.7	187±5	135±11	3.4±0.1	–	–	–
0.436	59.2	92	70±1	137±4	122±16	2.6±0.2	145±15	122±70	2.9±0.8
0.998	53.3	81	62±2	113±4	108±18	2.5±0.2	116±11	108±60	2.7±0.8
2.005	44.0	64	48±1	86±2	89±14	2.5±0.2	79±8	87±60	2.2±1
2.965	38.8	55	–	–			64±6	75±60	2. ±1
4.873	33.4	45					49±1	60±77	1.5±1.6
7.748	28.4	37							
10.21	25.5	33							
14.06	23.7	30							
17.47	22.4	28							
20.15	21.5	26							
42.17	19.0	21							

[a] From lineshape deconvolution.
[b] From eqs. 1 and 7.
[c] From eq. 6.
[d] From eqs. 6 and 7.

[NPr_4Br] (mM)	$1/T_1$ (s^{-1})	$1/T_2$ (s^{-1})	$1/T_{2s}$ [a] (s^{-1})	$1/T_{2f}$ [a] (s^{-1})	$\sqrt{p}\chi$ [b] (kHz)	τ_c (ns)	$1/T_{2f}$ [c] (s^{-1})	$\sqrt{p}\chi$ [d] (kHz)	τ_c [d] (ns)
0	65.1	102	73±0.6	188±4	136±10	3.4±0.1	–	–	–
0.991	62.4	96	73±1	151±4	128±13	3.7±0.1	–	–	–
1.961	55.2	87	65±1	124±3	114±54	3.6±0.8	143±14	116±60	3.2±0.8
2.969	53.1	81	64±2	104±4	108±22	2.1±0.3	117±12	108±64	2.7±0.9
4.033	49.3	75	58±1	100±2	101±12	2.4±0.2	107±11	101±60	2.8±0.9
6.121	46.2	66	53±1	88±3	91±16	2.5±0.3	80± 8	91±63	2.0±0.9
8.080	39.4	59	46±1	78±2	78± 8	2.9±0.2	67± 7	79±56	2.6±1
9.985	39.1	57	44±1	77±2	75±14	3.2±0.3	58± 6	76±61	2.2±1
12.89	36.8	52	40±1	72±2	64±16	4.2±0.5	57± 6	69±66	1.8±1.2
16.51	33.4	49	–	–		–	–	–	
19.96	37.7	44							
42.03	25.8	34							

[a] From lineshape deconvolution.
[b] From eqs. 1 and 7.
[c] From eq. 6.
[d] From eqs. 6 and 7.

[NBu_4Br] (mM)	$1/T_1$ (s^{-1})	$1/T_2$ (s^{-1})	$1/T_{2s}$ [a] (s^{-1})	$1/T_{2f}$ [a] (s^{-1})	$\sqrt{p}\chi$ [b] (kHz)	τ_c (ns)	$1/T_{2f}$ [c] (s^{-1})	$\sqrt{p}\chi$ [d] (kHz)	τ_c [d] (ns)
0.413	59	98	70±0.6	169±4	130±10	3.3±0.1	–	–	–
0.791	62	92	68±0.6	151±3	123± 9	3.1±0.1	150±15	118±14	2.8±0.1
1.091	59	91	66±0.9	134±4	120±14	2.7±0.2	148±15	120±50	3.2±0.7
1.597	56	86	–	–	–	–	121±12	113±50	2.6±0.6
2.047	56	78	–	–	–	–	98±10	108±35	1.9±0.6
2.689	50	72					90± 9	98±55	2.1±0.7
3.444	47	64					74± 7	93±58	1.5±0.8
5.079	39	57					68± 7	75±60	2.3±1
6.464	37	52					57± 6	68±68	1.8±1.3

Table 2 (continued)

[NBu_4Br] (mM)	$1/T_1$ (s^{-1})	$1/T_2$ (s^{-1})	$1/T_{2s}$ [a] (s^{-1})	$1/T_{2f}$ [a] (s^{-1})	$\sqrt{p}\chi$ [b] (kHz)	τ_c (ns)	$1/T_{2f}$ [c] (s^{-1})	$\sqrt{p}\chi$ [d] (kHz)	τ_c [d] (ns)
8.490	32	44						–	
10.24	32	44							
13.12	31	41							
16.04	26	36							
20.13	25	33							
42.34	21	28							

[a] From lineshape deconvolution.
[b] From eqs. 1 and 7.
[c] From eq. 6.
[d] From eqs. 6 and 7.

[NPe_4Br] (mM)	$1/T_1$ (s^{-1})	$1/T_2$ (s^{-1})	$1/T_{2s}$ [a] (s^{-1})	$1/T_{2f}$ [a] (s^{-1})	$\sqrt{p}\chi$ [b] (kHz)	τ_c (ns)	$1/T_{2f}$ [c] (s^{-1})	$\sqrt{p}\chi$ [d] (kHz)	τ_c [d] (ns)
0	67.5	105	74±0.6	191±5	137±11	3.4±0.1	–	–	–
0.210	65.1	98	72±0.6	168±4	131± 9	3.1±0.1	155±16	128±70	2.9±0.8
0.493	62.7	92	68±0.8	153±4	124±11	3.1±0.1	133±13	121±65	2.5±0.8
0.745	57.9	86	63±1.3	129±4	113±17	2.9±0.2	123±12	119±66	2.3±0.8
1.006	54.4	78	65±2	115±4	112±20	2.4±0.2	103±10	111±63	2.0±0.8
1.279	50.0	73	56±0.6	100±3	98±11	2.6±0.2	97±10	99±60	2.5±0.8
1.611	45.9	66	50±0.8	91±2	87±13	3.1±0.2	94± 9	90±60	3.0±1
2.067	42.9	60	–	–	–		79± 8	91±63	2.0±1
2.519	39.8	55	–	–	–		69± 7	84±66	1.8±1
3.096	35.4	49	–	–	–		–	–	–
3.997	31.9	42							
5.211	28.9	38							
10.97	23.6	28							

[a] From lineshape deconvolution.
[b] From eqs. 1 and 7.
[c] From eq. 6.
[d] From eqs. 6 and 7.

[NHe_4Br] (mM)	$1/T_1$ (s^{-1})	$1/T_2$ (s^{-1})	$1/T_{2s}$ [a] (s^{-1})	$1/T_{2f}$ [a] (s^{-1})	$\sqrt{p}\chi$ [b] (kHz)	τ_c (ns)	$1/T_{2f}$ [c] (s^{-1})	$\sqrt{p}\chi$ [d] (kHz)	τ_c [d] (ns)
0	62	104	73±0.6	195±6	137±13	3.6±0.1	–	–	–
0.091	62	101	71±0.8	187±6	134±14	3.5±0.2	–	–	–
0.162	58	94	65±0.5	172±4	125±10	3.7±0.1	164±16	123± 55	3.6±0.7
0.254	53	85	63±0.9	144±4	116±13	3.3±0.2	147±15	116± 60	3.5±0.8
0.315	52	81	60±0.6	126±3	109±10	3.1±0.1	131±13	110± 60	3.3±0.8
0.433	50	74	57±0.6	112±2	102± 9	3.0±0.1	96±10	105± 50	2.3±0.7
0.477	49	77	57±0.6	118±3	104±11	3.1±0.2	122±12	100± 60	3.3±0.8
0.511	46	70	52±0.6	109±3	96±11	3.4±0.2	96±10	95± 35	2.7±0.8
0.587	45	67	–	–	–	–	87± 9	90± 33	2.5±0.4
0.666	44	65	–	–	–	–	82± 8	90± 50	2.2±0.8
0.847	41	62					78± 8	82± 60	2.5±0.1
1.032	37	52					59± 6	107±110	0.6±0.9
1.276	34	46							

[a] From lineshape deconvolution.
[b] From eqs. 1 and 7.
[c] From eq. 6.
[d] From eqs. 6 and 7.

Table 2 (continued)

[NMe_3DoBr] (mM)	$1/T_1$ (s^{-1})	$1/T_2$ (s^{-1})	$1/T_{2s}$ [a] (s^{-1})	$1/T_{2f}$ [a] (s^{-1})	$\sqrt{p}\chi$ [b] (kHz)	τ_c (ns)	$1/T_{2f}$ [c] (s^{-1})	$\sqrt{p}\chi$ [d] (kHz)	τ_c [d] (ns)
0	64	98	71±0.5	190±4	134±25	3.6±0.3			
0.067	62	94	67±0.6	172±4	127±11	3.5±0.1			
0.144	56	88	64±0.6	149±3	119± 8	3.3±0.1			
0.263	53	77	57±0.6	115±3	103±10	3.1±0.1			
0.350	45	69	51±0.5	102±2	93± 8	3.3±0.1			
0.311	50	72	54±0.6	102±2	96± 9	3.0±0.1			
0.418	44	62	47±0.8	90±2	83±12	3.3±0.2			
0.479	41	58	43±0.6	82±2	75±12	3.8±0.3			
0.548	40	53	42±0.6	75±2	69±12	3.8±0.3			

[a] From lineshape deconvolution.
[b] From eqs. 1 and 7.
[c] From eq. 6.
[d] From eqs. 6 and 7.

tween two types of situations, 'free' Na^+ on the one hand, and Na^+ 'complexed' by DNA on the other. Then the apparent relaxation rates appearing in eq. 1a are [22]:

$$1/T_{2f} = \frac{p_F}{T_{2F}} + \frac{p_B}{T'_{2f}} \tag{7a}$$

$$1/T_{2s} = \frac{p_F}{T_{2F}} + \frac{p_B}{T'_{2s}} \tag{7b}$$

where p_F and p_B are the mole fractions of free and complexed Na^+, and where the relaxation rates $(T'_{2f})^{-1}$ and $(T'_{2s})^{-1}$ are given by eq. 1b and 1c, respectively. In analysing all our results, we have taken $p_F/T_{2F} = 30\ s^{-1}$; this allows us to determine from eqs. 1 and 7 the correlation time τ_c and the product $p_B^{1/2}\chi$, as given in table 2. We shall return to this hypothesis in section 4.

4. Discussion

Before proceeding further, one has to ascertain the meaning of finding sodium ions characterized by a correlation time $\tau_c = 3.4$ ns. This point remains controversial. Halle et al. [30] consider only free and atmospherically condensed sodium ions. They do not take into account site-bound sodium ions. One will recall that atmospherically condensed ions are loose, solvent-separated ion pairs [31]. Halle et al. [30] propose a dissociative relaxation mechanism: the sodium counterion diffuses out of the cylindrical cell [32], till it is able to enter another cylindrical cell, also occupied by a DNA molecule but differently oriented with respect to the laboratory axes. In such a model, the correlation time is related to the time for the random walk migration of the sodium ions from their old to the new environment. This exodus model has the merit of consistency with dilution experiments: τ_c increases as polymer concentration is reduced [17,19,25,26].

We remain unconvinced by this physical picture. Even though we do not have enough data to settle this question, we submit that a simpler tumbling model offers an alternative: it is sufficient for sodium ions to reorient freely, at their condensed positions, i.e., without escaping from the cylindrical cell they are in, to effect their nuclear relaxation. Such a reorientational motion modulates the efg-quadrupole moment interaction, and therefore should be considered as a prospective relaxation mechanism.

However, yet another picture accounts for the dilution experiments, in our opinion. The observed correlation time is due to site-bound rather than atmospherically condensed counterions. It is well known that polyelectrolytes gain flexibility with increasing ionic strength [33]. Site-bound sodium ions sample the motions of DNA (internal

and overall). As the polyelectrolyte molecule becomes a more and more rigid rod, τ_c for the associated sodium ions increases.

Despite our opinion on this point, we prefer to leave it unsettled: we shall use the measured product $p_B\chi^2$ as an empirical index of the mole fraction of sodium ions interacting with DNA, without attempting to pinpoint the nature of this interaction.

Addition of NaCl to the DNA solution reduces the relaxation rates (fig. 1). Deconvolution reveals that not only is the $p_B\chi^2$ term reduced, but also the correlation time τ_c, which decreases from 3.4 to 2 ns. Below this limit, we can detect only one component of the transverse magnetization, because the product $\omega_0\tau_c$ becomes smaller than unity. Yet the difference $(1/T_2 - 1/T_1)$ continues to decrease, till the conditions of extreme narrowing are fulfilled, when $\omega_0\tau_c \ll 1$ and the longitudinal and transverse relaxation rates are equalized.

Hence, rather than interpreting directly the changes in the linewidth as a measure of the fraction of complexed sodium ions, it is preferable to consider the product $p_B\chi^2$, in order to avoid contamination from the reduction in τ_c. That the mole fraction of complexed sodium ions p_B should decrease upon addition of NaCl to a DNA solution is typical of a polyelectrolytic solution. It maintains invariant the mole fraction of counterions neutralizing the electric charges on the polymeric sites. Such behavior escapes from mass action law [34], but is perfectly reproduced either by an accurate Poisson-Boltzmann treatment [14] or by an empirical model such as that of Manning [35–38] which has enjoyed widespread popularity.

We shall draw upon this feature for estimating

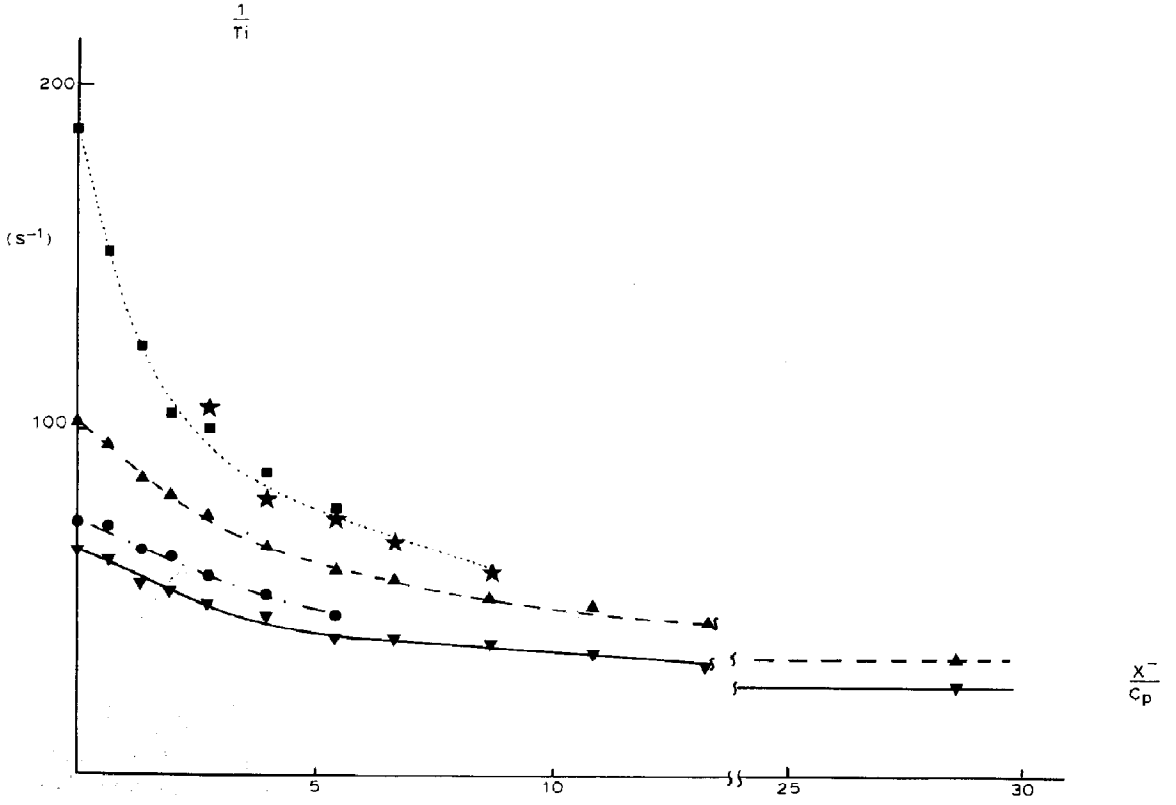

Fig. 2. Same as fig. 1, for addition of NPr_4Br.

the mole fraction of the surfactant counterions interacting with the DNA surface. For this purpose, we monitor the reduction of the product $p_B\chi^2$ (for sodium ions) as surfactant counterions are added to the DNA solution. Both types of counterions compete for neutralization of the charges on the biopolymer. The observed reduction denotes expulsion of sodium ions from the vicinity of DNA, as the quaternary ammonium ions enter.

The first type of results is obtained upon addition of NPr_4^+ to the NaDNA solution: the results are qualitatively similar to those from adding Na^+; the only difference is the quantity of salt, $NPr_4^+Br^-$ or Na^+Cl^-, necessary for the same reduction of the relaxation rates to be observed. The explanation is quite simple: the bulkier NPr_4^+ condenses less readily than Na^+ around the charged polyanion. Hence, a greater amount of the Q^+ salt will be necessary to displace the same quantity of sodium ions. Indeed, even when the ratio NPr_4^+/c_p is greater than 25, the ^{23}Na lineshape still fails to obey the extreme narrowing condition.

Let us now consider the entire series of Q^+ ions: if the DNA-counterion interactions were purely electrostatic, the above result should be totally general, and the quantity of salt required to displace the same fraction of complexed sodium ions should increase with the size of the Q^+ counterion, according to the sequence: $NPr_4^+ < NBu_4^+ < NPe_4^+ < NHex_4^+$. In fact, the observations run completely opposite to such a prediction. Furthermore, in the case of NMe_3Do^+, the surfactant-DNA interaction is very strong, to such an extent that it outweighs the Na^+-DNA interaction itself (fig. 3). This result, taken in itself, is indisputable proof of specific interactions – which one is

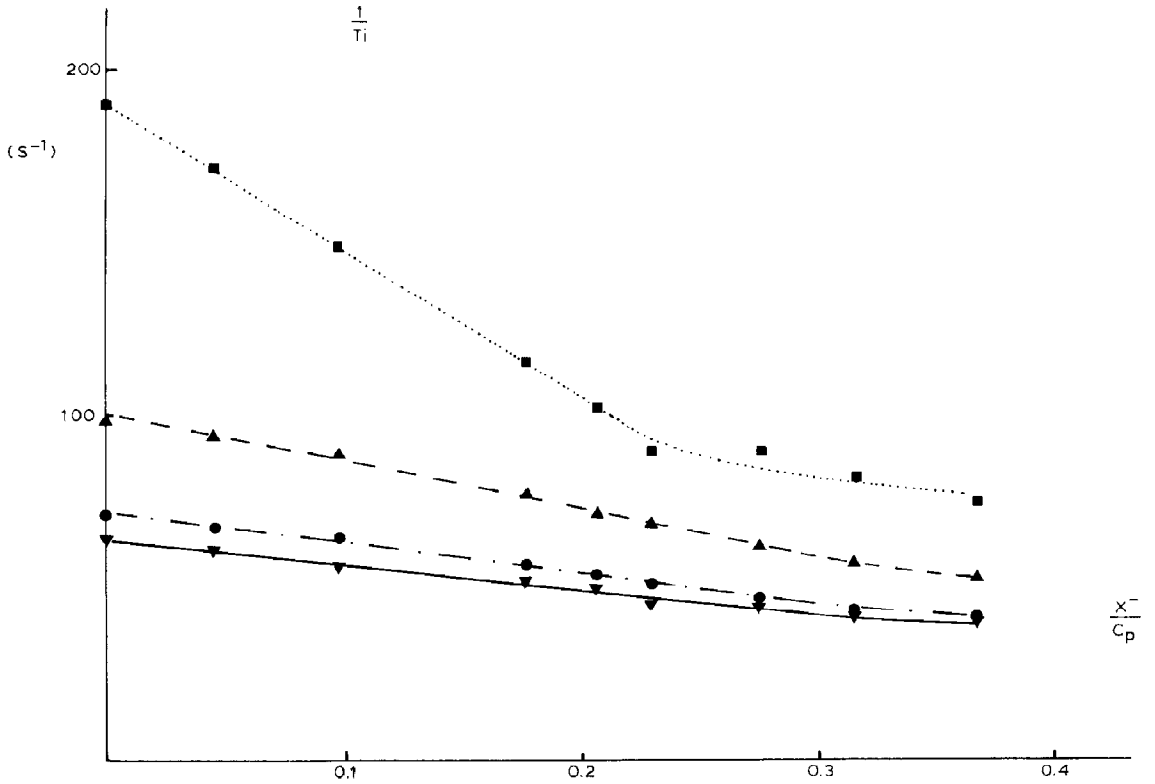

Fig. 3. Same as fig. 1, for addition of NMe_3DoBr.

strongly tempted to label as site-binding – between DNA and the surfactant counterion. The location of the interaction most probably is not the phosphate sites of the polyion.

These interactions, from the above sequence, bear a strong resemblance to what would result from operation of hydrophobic forces. The input of the positive charges is such as to neutralize the negative charges on the phosphate groups, thus reducing electrostatic attraction of the sodium ions. The contribution of the alkyl chains could favor a cooperative interaction of adjoining surfactant molecules bound on neighboring sites [6,7]. We cannot rule out intervention of other components of the DNA molecule in this interaction.

However, another explanation also cannot be ruled out: binding of the surfactant would change the conformation of DNA in such a way as to reduce accessibility of the phosphate sites to the sodium ions. Such conformational changes have been observed [4,39,40]. The number of surfactant molecules, though, required to induce such transitions is markedly greater [4,40] than in the present case, where there is less than one surfactant molecule per polymeric site. We shall return to this point later.

The other surfactants studied, viz. NBu_4^+, NPe_4^+ and NHe_4^+, display behavior intermediate between those of NPr_4^+ and of NMe_3Do^+. Rather than reproduce a whole series of curves entirely similar to those in figs. 2 and 3, we opt for a display of the mole fraction of complexed sodium ions: this parameter determines (together with the correlation time τ_c) the observed relaxation rates. Moreover, it provides quantitative information on the magnitude of the surfactant cation-DNA in-

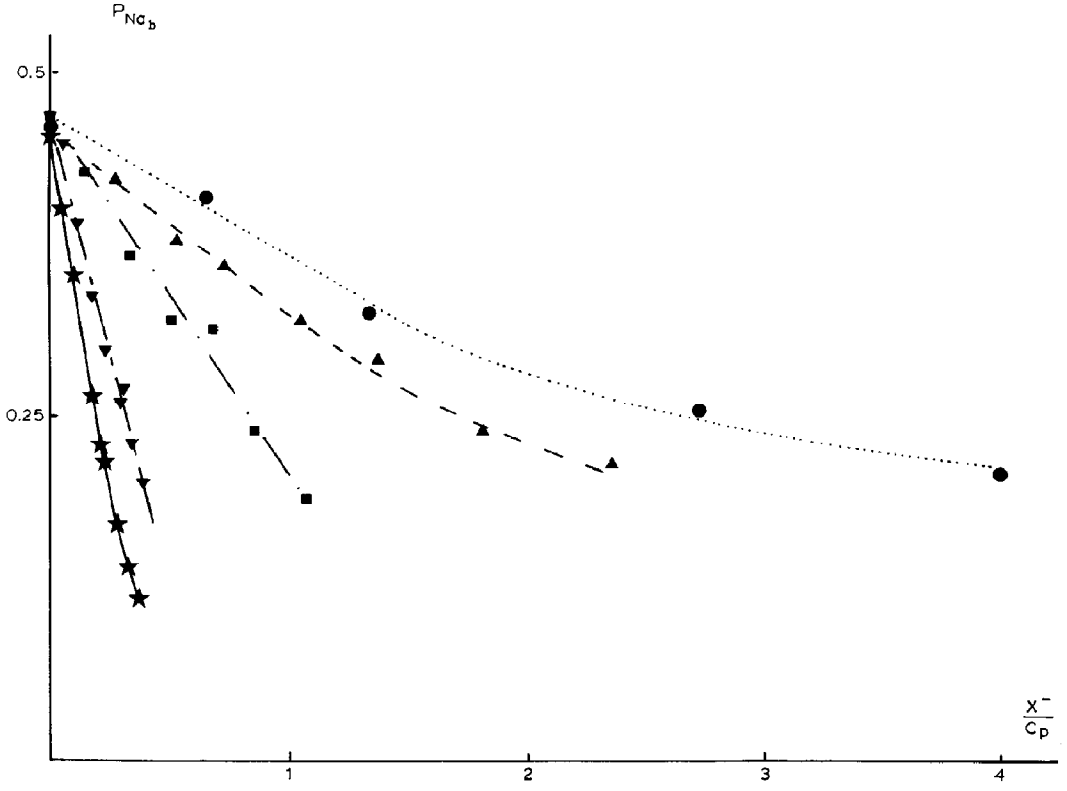

Fig. 4. Mole fraction of complexed sodium ions as a function of surfactant addition. (●) NPr_4^+, (▲) NBu_4^+, (■) NPe_4^+, (▼) NHe_4^+, (★) NMe_3Do^+. The curves shown are again merely for easier visualization.

teraction. Let us remind the reader that p_B results from two opposing tendencies, ionic condensation which favors the smallest Q^+ ions, and a hydrophobic binding favoring conversely the largest Q^+ ions.

As shown in fig. 4, the surfactant cation-DNA interaction grows with the length of the hydrocarbon chains, as expected for such a hydrophobic interaction. Already with the NBu_4^+ cation, the *n*-butyl chains are of sufficient length that the hydrophobic interaction due to this cation is significant. We had detected it, in an earlier companion study [41], from ^{59}Co data on salts of cobalt hexacyanide triple anion. Apparently, a highly charged anion [$Co(CN)_6^{3-}$ or $DNAP^-$] is necessary for this interaction to display itself, the anion increasing the local concentration of the Q^+ counterions around it, thus setting the hydrocarbon chains from two (or more) Q^+ ions into van der Waals contact. We have drawn fig. 4 for a quadrupolar coupling constant $\chi = 200$ kHz. This arbitrary choice, not unreasonable for ^{23}Na [10], does not lead to systematic errors if one sticks to relative comparisons as we are doing here. The only underlying assumption is that of a single mode of complexation (and of a single mode of relaxation) for the sodium counterions, unaltered upon binding of the surfactant ions by DNA. Both of these assumptions are difficult to assess, since little is known about either the locality of sodium ions bound to DNA or the character of the interactions that cause the quadrupolar relaxation. This assumption would fail if surfactant binding led to a conformational change of the DNA host.

We do not believe this to be likely since, even for the samples displaying a significant loss of solubility of the DNA (addition of NHe_4^+ and NMe_3Do^+), we have remained well below one surfactant molecule for two phosphate sites. Nevertheless, and in order not to introduce such an error, we shall limit consideration to the initial slopes for the various curves in fig. 4, related to the initial slope in an NaCl addition experiment.

The monotonic plot in fig. 5 is as expected for hydrophobic effect, increasing with the size of the cation surfactant. It shows a DNA-NMe_3Do^+ interaction greater than that of DNA-Na^+ by a

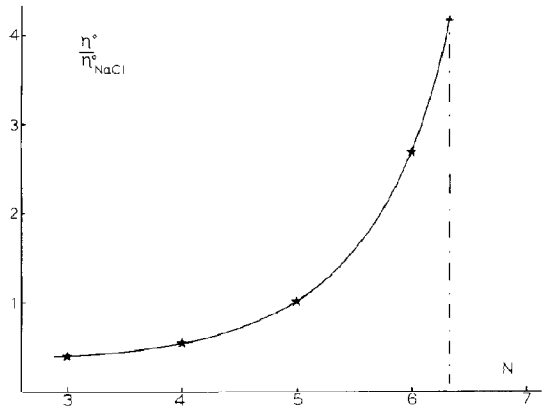

Fig. 5. Initial slopes, measured on fig. 4 and related to the initial slope in the addition of sodium chloride ($\eta^\circ_{NaCl} = 0.25$), as a function of the chain length (N = no. of carbons) for symmetrical tetraalkylammonium ions.

factor of 4. The point relative to the trimethyldodecylammonium ion, with its dissymetric structure, extrapolates to a symmetrical tetraalkylammonium with a chain length between 6 and 6.5, which appears as entirely reasonable.

All the results presented here stem from these working hypotheses:

(1) fast chemical exchange between two types of environment sampled by the sodium ions;

(2) a single correlation time τ_c descriptive of complexed sodium ions;

(3) the mode of complexation of sodium ions remains unaltered upon surfactant binding;

(4) likewise, χ characteristic of bound sodium ions remains invariant upon attachment of detergent Q^+ ions;

(5) use of a (p_F/T_{2F}) value of 30 s^{-1} in eq. 7.

We have made these hypotheses for simplicity's sake. The first two are sufficient to account for all of the observed relaxation rates. The next two (3 and 4) are made more legitimate by our exclusive reliance on initial slopes (figs. 4 and 5). We come now to justification of a (p_F/T_{2F}) value of 30 s^{-1} in eq. 7. Justification of a constant value, and of one greater than 17 s^{-1}, stems from the study of sodium polymethacrylate by Leyte et al. [42]: measurement of relaxation rates at different magnetic field strengths gave them a range of values for the (p_F/T_{2F}) term of 30–40 s^{-1} for charge

fractions varying between 5 and 50%. Furthermore, addition of salt to the polyelectrolyte solution reduces T_{2F}^{-1}, but it simultaneously increases p_F, the mole fraction of free ions: thus, the ratio p_F/T_{2F} approaches the limiting value 17 s^{-1}. Because of these two opposing trends, and because of the attendant simplification, we have chosen to consider the (p_F/T_{2F}) term as constant.

Why give it a value of 30 s^{-1}? So that it be greater than 17 s^{-1}, smaller than an upper limit of approx. 40 s^{-1}, and so that it conforms to the range found by Leyte et al. [42]. This choice is not crucial. Changing the value from 30 to 17 s^{-1} amounts to a 10% maximum change of $p^{1/2}\chi$ and to a less than 15% variation of τ_c. And, yet more important, our qualitative conclusions about the sequence of affinities of the various Q^+ ions for DNA will remain unaffected because they are based only on relative comparisons of the initial slopes in fig. 5.

The one sore point is the absence of an adequate theory, which has prevented us from further analysis of the experimental results: we do not know if the observed τ_c describes the mobility of the phosphate-binding sites, or the mobility of sodium ions condensed in the electrostatic atmosphere surrounding the DNA macromolecule.

5. Conclusions

^{23}Na-NMR [10,11] has once more proven its worth for the study of interactions between a polyelectrolyte and surfactant counterions. It has allowed us here to show the existence of a strong, specific interaction, of obvious hydrophobic origin. Deconvolution of the lineshapes allowed precise quantitation of these interactions, by comparison to a reference cation, the sodium ion.

Acknowledgments

We thank Mr. Eric Dandois for the DABA determinations. We also thank Dr. Eric Enwall (University of Oklahoma, Norman) for letting us use his minimization program. We gratefully acknowledge Professeurs Eugène Frédéricq and Claude Houssier (laboratoire de chimie physique, Université de Liège) and Professeur Albert Distèche (laboratoire d'océanologie, Université de Liège) for access to viscosimetry and atomic absorption spectrophotometry (Perkin Elmer 370A) apparatus. We are indebted to Fonds National de la Recherche Scientifique and to Programmation de la Politique Scientifique (Action Concertée 82/87-34), Brussels, for grants for purchase of the Bruker AM 300 WB NMR spectrometer. The manuscript was prepared while one of us (P.L.) benefited from the hospitality of the Institute of Molecular Science, in Okazaki, Japan. A.D. is chargé de recherche FNRS.

References

1 H.S. Hanna and P. Somasundaran, J. Colloid. Interface Sci. 70 (1979) 181.
2 K. Shirahama, H. Yuasa and S. Sugimoto, Bull. Chem. Soc. Jap. 54 (1981) 375.
3 T. Isemura and A. Imanishi, J. Polym. Sci. 33 (1958) 337.
4 I. Satake, T. Gondo and H. Kimizuka, Bull. Chem. Soc. Jap. 52 (1979) 361.
5 K. Hayakawa and J.C.T. Kwak, J. Phys. Chem. 86 (1982) 3866.
6 K. Hayakawa, J.P. Santerre and J.C.T. Kwak, Biophys. Chem. 17 (1983) 175.
7 A. Delville, Chem. Phys. Lett. 118 (1985) 617.
8 A. Delville, Biophys. Chem. 19 (1984) 183.
9 D. Poland, Cooperative equilibria in physical biochemistry (Clarendon Press, Oxford, 1978).
10 P. Laszlo, Angew. Chem. 90 (1978) 271; Angew. Chem. Int. Ed. Engl. 17 (1978) 254.
11 P. Lazslo, in: NMR spectroscopy: New methods and applications, ed. G.C. Levy, ACS Symposium Series no. 191 (American Chemical Society, Washington, 1982) p. 63.
12 R.A. Marcus, J. Chem. Phys. 23 (1955) 1057.
13 G. Gunnarsson and H. Gustavsson, J. Chem. Soc. Faraday Trans. I, 78 (1982) 2901.
14 A. Delville and P. Laszlo, Biophys. Chem. 17 (1983) 119.
15 A. Delville, L. Herwats and P. Laszlo, Nouv. J. Chim. 8 (1984) 557.
16 C.F. Anderson, M.T. Record, Jr and P.A. Hart, Biophys. Chem. 7 (1978) 301.
17 M.L. Bleam, C.F. Anderson and M.T. Record, Jr. Proc. Natl. Acad. Sci. U.S.A. 77 (1980) 3085.
18 M. Levij, J. de Bleijser and J.C. Leyte, Bull. Magn. Reson. 2 (1980) 388.
19 M.L. Bleam, C.F. Anderson and M.T. Record, Jr, Biochemistry 22 (1983) 5418.
20 L. Nordenskiold, D.K. Chang, C.F. Anderson and M.T. Record, Jr, Biochemistry 23 (1984) 4309.

21 J.J. van der Klink, L.H. Zuiderweg and J.C. Leyte, J. Chem. Phys. 60 (1974) 2391.
22 H. Gustavsson, B. Lindman and T. Bull, J. Am. Chem. Soc. 100 (1978) 4655.
23 B. Meurer, P. Spegt and G. Weill, Chem. Phys. Lett. 60 (1978) 55.
24 S.W.T. Westra and J.C. Leyte, Ber. Bunsenges. Phys. Chem. 83 (1979) 678.
25 M. Levij, J. de Bleijser and J.C. Leyte, Chem. Phys. Lett. 83 (1981) 183.
26 A. Delville, H. Gilboa and P. Laszlo, J. Chem. Phys. 77 (1982) 2045.
27 J. Eigner and P. Doty, J. Mol. Biol. 12 (1965) 549.
28 P.S. Hubbard, J. Chem. Phys. 53 (1970) 985.
29 A. Delville, C. Detellier and P. Laszlo, J. Magn. Reson. 34 (1979) 301.
30 B. Halle, H. Wennerstrom and L. Piculell, J. Phys. Chem. 88 (1984) 2482.
31 M. Szwarc, Ions and ion pairs in organic reactions, vol. 1 (Wiley, New York, 1971).
32 R.M. Fuoss, A. Katchalsky and S. Lifson, Proc. Natl. Acad. Sci. U.S.A. 37 (1951) 579.
33 T. Odijk, Macromolecules 12 (1979) 688.
34 S. Forsén and B. Lindman, Methods Biomed. Anal. 27 (1981) 229.
35 G.S. Manning, J. Chem. Phys. 51 (1969) 924.
36 G.S. Manning, Biophys. Chem. 9 (1978) 65.
37 G.S. Manning, Acc. Chem. Res. 12 (1979) 443.
38 G.S. Manning, J. Phys. Chem. 85 (1981) 877.
39 M.J. Grourke and J.H. Gibbs, Biopolymers 5 (1967) 586.
40 I. Satake and J.T. Yang, Biopolymers 15 (1976) 2263.
41 A. Delville, A. Stockis and P. Laszlo, J. Am. Chem. Soc. 103 (1981) 5991.
42 C.W.R. Mulder, J. de Bleijser and J.C. Leyte, Chem. Phys. Lett. 69 (1980) 354.